Gene expression profiling of microdissected Hodgkin Reed-Sternberg cells correlates with treatment outcome in classical Hodgkin lymphoma

Christian Steidl,[1,2] Arjan Diepstra,[3] Tang Lee,[1] Fong Chun Chan,[1,4] Pedro Farinha,[1] King Tan,[1] Adele Telenius,[1] Lorena Barclay,[5] Sohrab P. Shah,[2] Joseph M. Connors,[1] Anke van den Berg,[3] and Randy D. Gascoyne[1,2]

[1]Centre for Lymphoid Cancer, British Columbia Cancer Agency, Vancouver, BC; [2]Department of Pathology and Laboratory Medicine, University of British Columbia, Vancouver, BC; [3]Departments of Pathology and Medical Biology, University of Groningen, University Medical Center, Groningen, The Netherlands; [4]Bioinformatics Training Program, University of British Columbia, Vancouver, BC; and [5]Department of Cancer Imaging, British Columbia Cancer Agency, Vancouver, BC

In classical Hodgkin lymphoma (CHL), 20%-30% of patients experience relapse or progressive disease after initial treatment. The pathogenesis and biology of treatment failure are still poorly understood, in part because the molecular phenotype of the rare malignant Hodgkin Reed-Sternberg (HRS) cells is difficult to study. Here we examined microdissected HRS cells from 29 CHL patients and 5 CHL-derived cell lines by gene expression profiling. We found significant overlap of HL-specific gene expression in primary HRS cells and HL cell lines, but also differences, including surface receptor signaling pathways. Using integrative analysis tools, we identified target genes with expression levels that significantly correlated with genomic copy-number changes in primary HRS cells. Furthermore, we found a macrophage-like signature in HRS cells that significantly correlated with treatment failure. CSF1R is a representative of this signature, and its expression was significantly associated with progression-free and overall survival in an independent set of 132 patients assessed by mRNA in situ hybridization. A combined score of CSF1R in situ hybridization and CD68 immunohistochemistry was an independent predictor for progression-free survival in multivariate analysis. In summary, our data reveal novel insights into the pathobiology of treatment failure and suggest CSF1R as a drug target of at-risk CHL. (*Blood*. 2012; 120(17):3530-3540)

Introduction

Hodgkin lymphoma (HL) is the most common lymphoid cancer in patients younger than 40 years. Despite modern treatment strategies resulting in significantly improved overall survival (OS), ~ 20% of patients with classical Hodgkin lymphoma (CHL) die because of progressive disease. Although targeted therapies for HL are emerging,[1,2] a more detailed molecular inventory of HL is needed to better understand the pathogenesis of the disease and in particular the biological correlates of treatment failure.

CHL is unique among lymphomas because of the paucity of the malignant Hodgkin Reed-Sternberg (HRS) cells that are derived from clonal germinal center B cells.[3] Investigations of clinical cases using laser capture microdissection have allowed a more detailed analysis of the malignant HRS cells separate from the tumor microenvironment, including studies investigating copy number, gene expression profiling (GEP), and mutational analysis of target genes.[4-7] Seminal GEP studies using HL cell lines and a limited number of primary tissue samples established a molecular profile of nodular lymphocyte predominant HL and CHL that clearly distinguished HL from related entities and established a molecular link to primary mediastinal B-cell lymphoma.[8-11] However, these gene expression studies were limited by small case numbers and lack of available clinical data. Furthermore, it remains an open question whether commonly available HL cell lines are an accurate representation of clinical disease.

In recent years, the importance of the tumor microenvironment has shifted into focus for HL pathogenesis and outcome prediction.[12] However, it is still largely unknown whether certain molecular features of the malignant HRS cells are linked to the specific composition of the tumor microenvironment. In particular, certain T-cell subsets and tumor-associated macrophages were described as prognostic factors in patients treated with systemic ABVD (doxorubicin, bleomycin, vinblastine, and dacarbazine)-type chemotherapy.[13-15] Although these studies have not yet penetrated clinical practice, inclusion of biologic markers into risk assessment scores, such as the International Prognostic Factor Score,[16] is anticipated to change clinical management in favor of more individualized and targeted treatment approaches in the near future.[17]

To better characterize the gene expression features of primary HRS cells found in tissue samples, we analyzed 29 primary lymph node biopsies of CHL and 5 HL cell lines and found significant overlap but also differences in the gene expression profiles. Comparing gene expression profiles of treatment outcome groups (treatment failure vs success), we identified a signature of macrophage function in HRS cells that was correlated with first-line treatment failure. Expression of *CSF1R*, as a representative gene of this signature, was validated as an adverse prognostic marker in an independent cohort using mRNA in situ hybridization (ISH). These

Submitted June 27, 2012; accepted August 19, 2012. Prepublished online as *Blood* First Edition paper, September 5, 2012; DOI 10.1182/blood-2012-06-439570.

The online version of this article contains a data supplement.

The publication costs of this article were defrayed in part by page charge payment. Therefore, and solely to indicate this fact, this article is hereby marked "advertisement" in accordance with 18 USC section 1734.

Table 1. Clinical and pathologic characteristics of 29 patients with CHL studied by GEP of microdissected HRS cells

	Treatment success (no progression or relapse)	Treatment failure (progression or relapse)	*P*
N	15	14	
Median age, y	41	35	NS
Sex, male, %	60	72	NS
Histology			NS
Nodular sclerosis	14	12	
Mixed cellularity	1	2	
Lymphocyte-rich	0	0	
Lymphocyte-depleted	0	0	
NOS (not classifiable)	0	0	
Stage, %			.082
I	13	0	
II	60	29	
III	20	43	
IV	7	29	
B-symptoms, %	13	43	.075
Median mass size, cm	6.6	6.6	NS
≥ 10 cm, %	27	29	NS
High risk, IPS ≥ 4, %	20	14	NS
Primary treatment			NS
ABVD type ± radiation, %	93	93	
Extended field radiation alone, %	7	7	

NS indicates not significant.

data add further evidence to the importance of macrophage-related and CSF1R-dependent signaling in CHL. Our data suggest the HRS cell-macrophage interface as a promising drug target for at-risk CHL.

Methods

Patient samples

For the GEP study of microdissected HRS cells, biopsy material from 29 patients with CHL were selected from the tissue archive of the Centre for Lymphoid Cancer at the British Columbia Cancer Agency according to the following criteria: (1) confirmed diagnosis of HIV-negative CHL, (2) availability of fresh-frozen lymph node biopsies, (3) presence of sufficient numbers of HRS cells in the tissue sections used for microdissection, (4) availability of clinical outcome data, and (5) first-line treatment with systemic chemotherapy ABVD. The cohort included biopsies taken at relapse in 5 patients whose primary treatments failed. The clinical and pathologic characteristics of this GEP cohort are summarized in Table 1. There were no differences in any recorded clinical and pathologic parameters between the outcome groups, although a nonsignificant trend toward higher stages and occurrence of B symptoms in the treatment failure group were noted. Copy number changes and clinical outcomes of these 29 patients have been reported as part of a larger cohort that was previously published.[18]

Furthermore, gene expression of target genes was studied by ISH and immunohistochemistry (IHC) in an independent validation cohort of 166 pretreatment formalin-fixed, paraffin-embedded tissue biopsies of CHL. Clinical characteristics and outcomes of this patient cohort enriched for events and disease-specific deaths have been previously reported.[15] The clinical characteristics of the 132 patients evaluable by ISH are shown in Table 2.

Ethical approval for this study, conducted in accordance with the Declaration of Helsinki, was obtained from the University of British Columbia-British Columbia Cancer Agency Research Ethics Board (UBC BCCA REB #H07-02101).

Laser microdissection, cell culture, and RNA extraction

Laser capture microdissection was performed as previously described using a Zeiss Axioplan 2 microscope equipped with Molecular Machines Industries Technology.[18] In brief, 6-μm fresh frozen tissue sections were fixed in 70% ethanol and mounted onto membrane slides. Adjacent sections were also prepared on glass slides and stained with hematoxylin and eosin to assess cell morphology and HRS cell content. Sections mounted on membrane slide for microdissection were briefly stained with hematoxylin for 20 seconds, and 1000 individually picked cells per case were cut and lysed using RLT-Buffer (QIAGEN). Lysates were supplemented with carrier RNA (bacterial 16S- and 23S- ribosomal RNA, 4 μg/μL, Roche Diagnostics) and RNA extracted using QIAGEN RNeasy Micro kits (QIAGEN).

The human cell lines KM-H2, L428, L540, L1236, and HDLM2, derived from patients with HL, were obtained from the German Collection of Microorganisms and Cell Cultures (DSMZ). Cell lines were grown according to the standard conditions (http://www.dsmz.de/). RNA was extracted form early-passage cultures using Allprep extraction kits (QIAGEN).

We used 5 microdissected germinal centers of reactive tonsil specimens and 5 magnetically enriched $CD77^+$ centroblast specimens as controls for gene expression studies of clinical cases and cell lines, respectively. Magnetically activated cell sorting was performed by Miltenyi technology as previously described.[19]

GEP and data analysis

The comparison and analysis pipeline of the GEP experiments are shown in supplemental Figure 1 (available on the *Blood* Web site; see the Supplemental Materials link at the top of the online article). Gene expression profiles were obtained using GeneChip HG 133 Version 2.0 plus arrays (Affymetrix) after 2-cycle labeling reactions following the standard protocol (Affymetrix Genechip protocol). Data are available at www.ncbi.nlm.nih.gov/geo/query/acc.cgi (accession no. GSE39132, GSE39133, and GSE39134). For the microdissected specimens, all of the extracted RNA was used to prepare biotinylated cRNA; for the cell lines and magnetically enriched cells, the input was 10 ng. Labeled cRNA was then hybridized on the array overnight, and the arrays were washed, stained, and scanned using Affymetrix Fluidics Station 450 and Affymetrix GeneChip Scanner. Affymetrix gene expression data were preprocessed and normalized by Robust Multichip Average in R using Bioconductor.[20] All 44 reported microarrays passed the quality control criteria of present call rates $> 20\%$ and normalized unscaled standard errors < 1.05 (supplemental Figure 2). The expression profiles of

Table 2. Clinical characteristics of validation cohort used for mRNA ISH (N = 132)

	$CSF1R^-$ ISH	$CSF1R^+$ ISH	*P*
N (%)	69 (52)	63 (48)	
Median age, y (range)	35 (15-80)	43 (16-77)	NS
Sex, male, no. (%)	49	57	NS
Histology, %			.003
Nodular sclerosis	97	81	
Other	3	19	
Stage, %			NS
I	9	5	
II	54	44	
III	23	29	
IV	14	22	
B-symptoms (%)	39	54	NS
Median mass size, cm	8.0	6.9	NS
≥ 10 cm, (%)	35	29	NS
Treatment			NS
ABVD type ± radiation (%)	100	98	
Extended field radiation alone (%)	0	2	
$CD68^-$ IHC elevated ($CD68^+ > 5\%$)	65	83	.030

NS indicates not significant.

the 5 HL-derived cell lines and 5 centroblast samples have been previously reported by our group.[19]

Differentially expressed genes between analysis groups (supplemental Figure 1) were identified using 2-sample t-statistics (Bioconductor) and fold change. Raw *P* values and false discovery rate adjusted *P* values according to Benjamini and Hochberg were reported.[21] Overrepresentation and pathway analysis were performed using Ingenuity Pathway Analysis (Ingenuity Systems; www.ingenuity.com) studying overexpressed and underexpressed genes separately. Associative testing of gene signatures related to the group comparisons was performed using Globaltest Version 4.6.0 (Bioconductor). Principal component analysis was performed using the function plotPCA in the Affycoretools package (Bioconductor).

Immunohistochemistry and mRNA in situ hybridization on tissue microarrays

To validate expression and outcome correlations of specific gene targets, we studied 166 CHL patients on a tissue microarray constructed with 1.5-mm duplicate cores containing representative areas of HRS cells. For IHC, we used routine protocols for automated procedures on the Ventana Benchmark XT (Ventana Medical Systems). The following antibodies were used for reference staining: CD20 (Dako North America; L26), CD3 (polyclonal; Cell Marque), CD30 (Dako; Ber-H2), and CD68 (Dako; KP-1). Moreover, available formalin-fixed, paraffin-embedded tissues of cases of the GEP cohort (n = 24) were stained for granzyme B (GrB) (DAKO; GrB-7) and TNFRSF11A (RANK, R&D Systems; clone 80707) to validate mRNA expression findings. For mRNA ISH, we used a *CSF1R* PCR product that was subcloned in the pCRII-TOPO vector (Invitrogen) according to the instructions of the manufacturer. Primers for *CSF1R* used were 5′-CGCTTCCAAGAATTGCATCC-3′ (forward) and 5′-TCGGCA-GATTGGTATAGTCC-3′ (reverse). Orientation of the PCR product was determined by PCR using CSF1R specific primers in combination with vector-specific M13F and M13R primers. Sense and antisense DIG-labeled RNA probes were made with the DIG RNA labeling Kit (Sp6/T7; Roche Diagnostics). ISH was performed on paraffin-embedded sections using standard laboratory protocols.[22] Cases were only scored if the β-actin control and macrophages and plasma cells in the microenvironment were ISH-positive; all other cases were considered technical failures. ISH staining was scored by AD, and CSF1R-positive cases were defined by moderate to strong staining of HRS cells. The latent EBV infection status of HRS cells in the 24 cases of the GEP cohort with available formalin-fixed paraffin-embedded tissues was determined by ISH for EBV-encoded small RNA and scored by KT and RDG following routine clinical protocols. IHC and ISH images were acquired on a Nikon Eclipse E600 with 400× magnification equipped with a Nikon DS-Fi1.

Integrative copy number/gene expression analysis

Genome-wide copy number (CN) data were available for all 29 CHL cases as published.[18] Ensembl gene models were used to derive gene-specific CN values matched to gene expression (GE) values. Specifically, data were linked to genes as follows: (1) Genes were assigned CN values of either a single BAC probe (if fully or partially overlapping with a single genomic BAC alignment) or the average of adjacent BACSs (if overlapping with multiple genomic BAC alignments). Genes with no BAC coverage were eliminated from analysis. (2) Genes were directly assigned GE values if interrogated by a single probe set, or by averaging the hybridization intensities of multiple probe sets interrogating the same gene. The correlation of CN and GE values was performed using Spearman correlation on the 29 CN-GE pairs. Correlations were considered significant if $P < .05$.

Statistical analysis

Comparisons of clinical, IHC, and ISH parameters were performed by χ^2 and Student *t* tests. Previously reported CD68 IHC results[15] were included into the analysis and compared with CSF1R ISH results (χ^2 test). A combined score of CD68 (positivity in microenvironment cells) and CSF1R (positivity in HRS cells) was developed for clinical outcome analysis: $CD68^+/CSF1R^+$ score 2, $CD68^+/CSF1R^-$ or $CD68^-/CSF1R^+$ score 1, and $CD68^-/CSF1R^-$ score 0. For time to event analyses, we used progression-free survival (PFS, defined as the time from initial diagnosis to progression at any time, relapse from complete response, or initiation of new previously unplanned treatment) and OS (the time from initial diagnosis to death of any cause) as endpoints. Cox proportional hazard models and time to event analyses using the Kaplan-Meier method were performed using SPSS Software Version 11.0.0. Two-sided *P* values $< .05$ were reported as significant.

Results

GEP of microdissected HRS cells defines a CHL-specific expression pattern

To define a CHL-specific expression signature representative of primary CHL biology, we investigated microdissected HRS cells of 29 cases. Compared with gene expression profiles of microdissected reactive germinal center cells, we found 1342 significantly differentially expressed probe sets (group comparison fold change > 5, false discovery rate-adjusted $P < .001$), of which 382 probe sets were found to be up-regulated and 960 probe sets were down-regulated (supplemental data: Comparison gene lists) allowing for a clear separation between both experimental groups based on principle component analysis (supplemental Figure 3A). Of the 1342 probe sets, we used the 200 probe sets with the highest variance (supplemental Table 1) for unsupervised hierarchical clustering (Figure 1A). By doing so, we were able to define 3 separate clusters characterized by relative overexpression of genes representative of: (A) a cytotoxic immune response (eg, *GZMB*, *CXCL10*, and *C1Q*), (B) surface receptor signaling (eg, *TNFRSF11A*, *IL26*, *IL9*, *CCL17*, *PERP*, *CCND2*, and *TGFBR3*), and, (C) a B-cell signature (eg, *HLA-C*, *IGJ*, *IGHG3*, *IGL*, *AMIGO2*, and *PUO2AF1*). Using immunohistochemistry, we were able to demonstrate high protein expression of GrB and RANK in selected cases with high expression of GZMB and TNFRSF11A mRNA expression, respectively (Figure 1A), thus validating the GEP data and previous reports of cytotoxic molecule expression and TNF receptor signaling in HRS cells.[23,24] The 5 relapse biopsies did not cluster separately and were therefore included in the subsequent analyses. Gene set enrichment analysis using the differentially expressed genes in HRS cells compared with germinal center cells found overrepresentation of critically deregulated functions and pathways characteristic of CHL (Table 3). Most strikingly, genes involved in the cellular functions of apoptosis, surface receptor signaling, chemotaxis, lymphocyte proliferation, connective tissue proliferation, and cytotoxicity were overexpressed in HRS cells. These pathways included NF-κB signaling, JAK-STAT signaling, and interleukin signaling (Table 3). Significantly down-modulated cellular functions of HRS cells encompassed B-cell activation, antibody response, gene transcription, and the pathways of B- and T-cell receptor signaling, integrin signaling, IGF-1 signaling, and insulin receptor signaling (Table 4). For 24 of the 29 GEP cases, we were able to determine the EBV status of the HRS cells by ISH (7 cases EBV^+, 17 cases EBV^-). Using supervised analysis comparing the EBV^+ with EBV^- cases, we found 163 differentially expressed probe sets (group comparison fold change > 2, raw $P < .05$), of which 91 probe sets were down-regulated and 72 probe sets were up-regulated in EBV^+ cases (supplemental data: Comparison gene lists). Of note, among the up-regulated genes in EBV^+ cases were *CCL8*, *PERP*, *CD44*,

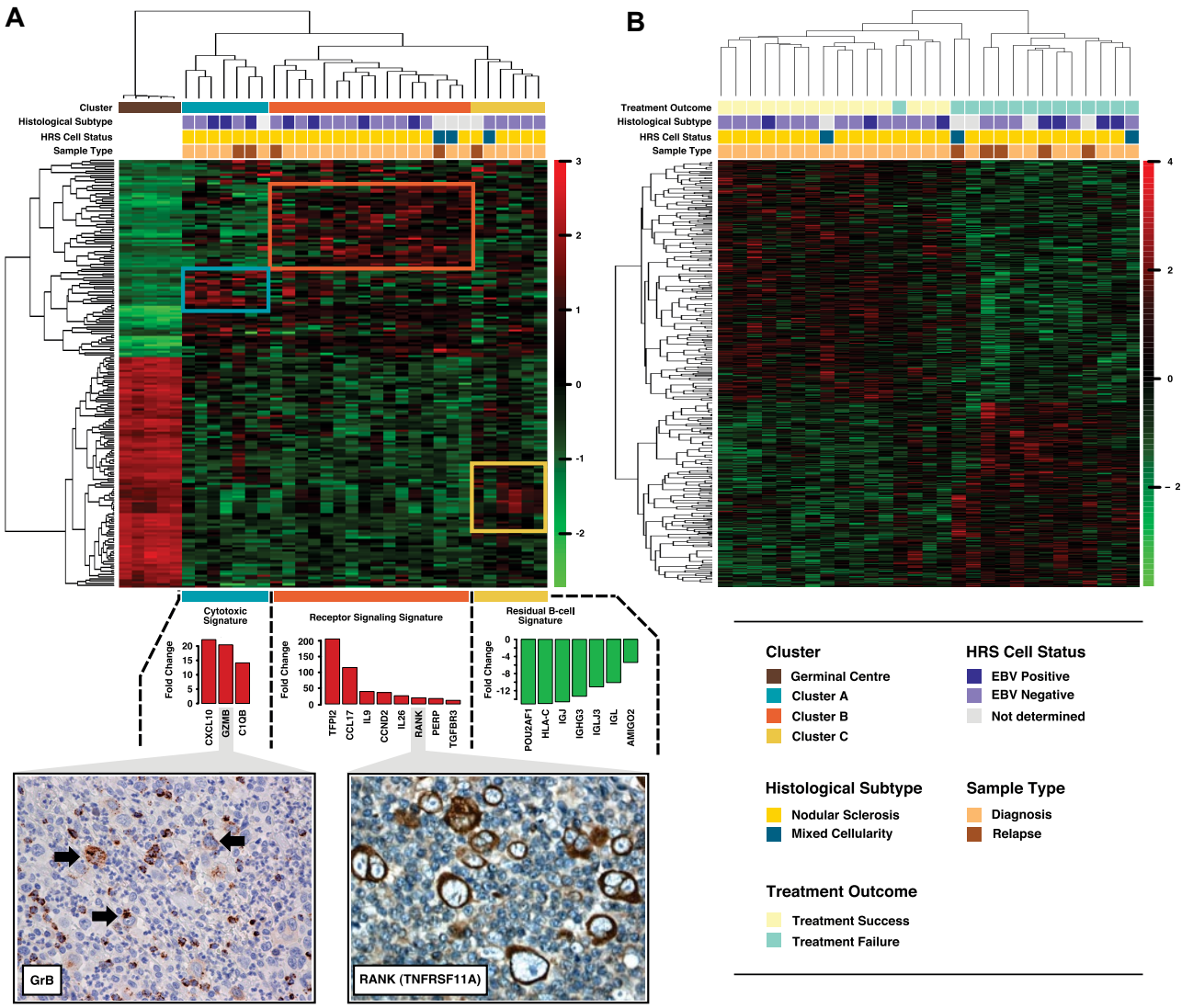

Figure 1. Expression profiling of 29 samples of microdissected HRS cells. (A) Unsupervised hierarchical cluster of 29 gene expression profiles is shown using the 200 genes with the highest variance. Red represents relative overexpression; and green, relative underexpression. Patient clusters, histologic subtype, EBV positivity of HRS cells by for EBV-encoded small RNA in situ hybridization, and sample type are shown. The average fold changes of genes representative of the 3 main signatures are shown in the bar plots. Representative immunohistochemistry images are depicted demonstrating cytoplasmic positivity of GrB (black arrows) and RANK in HRS cells. (B) Unsupervised hierarchical clustering of the cohort using the 200 most differentially expressed genes between primary treatment failure and success. Treatment outcome, histologic subtype, EBV positivity of HRS cells by for EBV-encoded small RNA in situ hybridization, and sample type are shown. Cases cluster according to the outcome groups (2 main clusters). Differentially expressed genes are given in the supplementary data (comparison gene lists).

TNFAIP3, *MAPK1*, *LMO2*, and *HOXB7*, and among the down-regulated genes *IL9*, *SATB1*, *TGFBR3*, *CX3CL1*, *WNT2*, *NTRK3*, *CD69*, *SPIB*, and *MAF*.

The gene expression profiles of microdissected HRS cells partially overlap with gene expression profiles of HL cell lines

GEP of HL-derived cell lines have been previously described and have significantly contributed to the understanding of HRS cell biology.[10,25] Here we compared the expression profiles of microdissected primary HRS cells with those of the cell lines to investigate both overlap and differences. Comparing gene expression profiles of the 5 commonly used HL-derived cell lines KM-H2, L-428, L-540, and L1236 with enriched $CD77^+$ centroblasts, we found 1004 significantly differentially expressed probe sets (group comparison fold change > 5, false discovery rate-adjusted $P < .001$), of which 169 probe sets were found to be up-regulated and 835 probe sets to be down-regulated (supplemental data: Comparison gene lists and supplemental Figure 4). A total of 26 annotated genes were overexpressed and 222 annotated genes underexpressed in both primary HRS cells and cell lines (supplemental Results). This overlap was statistically highly significant ($P < .00001$; supplemental Figure 3C-D). Comparable with primary HRS cells, the cell lines showed up-regulation of apoptosis, leukocyte proliferation, NF-κB signaling, and interleukin signaling (supplemental Table 2) and down-modulation of B-lymphocyte activation and signaling (supplemental Table 3). Importantly, although we found a significant overlap, many of the cellular functions and pathways discovered in primary HRS cells, such as chemotaxis and surface receptor signaling, including JAK-STAT signaling, remained undetected, highlighting also the significant differences in gene expression programs and emphasizing the value of HRS cell profiling from primary CHL cases.

Table 3. Function and involved pathways of genes up-regulated in HRS cells (Ingenuity Pathway Analysis)

	P (adjusted)	Molecules
Function annotation		
Adhesion of leukocytes	.0002	CD44, THY1, HGF, IL6, IL15, CCL5, CCL17, CCL19, CCL22, CX3CL1, TXN
Apoptosis of eukaryotic cells	.0000	TNFAIP3, TGFBR3, TNFRSF8, TNFRSF11A, GZMB, WNT2, WT1, TXN, ATF3, B2M, CCL5, CCND2, CD44, CD274, CDKN1A, CRH, CX3CL1, DUSP4, FBXO32, HGF, HOXC6, ID2, IER3, IL6, IL9, IL15, JUN, MAOA, MT2A, MUC1, NFKBIA, NTRK3, PDGFRA, PHLDA1, PLAT, PRAME, RASSF4, RTN1, SOCS3, STAT1, STAT5A, TRA@,
Cell surface receptor linked signal transduction	.0003	IL2RA, PDGFRA, CD274, COL3A1, CX3CL1, CXCL10, IL6, IL31RA, LILRB2, NTRK3, PTPRG
Chemotaxis of leukocytes	.0003	CCL5, CCL8, CCL17, CCL19, CCL22, CCR7, CX3CL1, CXCL10, IL15, SERPINA1, SOCS3, TXN
Cytotoxicity of eukaryotic cells	.0008	GZMB, CX3CL1, CCL5, TXN, IL15, STAT1, TNFAIP3, TNFRSF8,
Differentiation of leukocytes	.0000	TBX21, ID2, JUN, JUNB, TNFRSF11A, RORA, RORC, IL13RA2, IL6, IL9, IL15, IL2RA, TRA@, SOCS3, STAT1, STAT5A
Growth of eukaryotic cells	.0000	CDKN1A, STAT1, STAT5A, TGFBR3, HGF, CRH, CCND2, PTP4A3, PTPRG, NTRK3, ADCY1, ATF3, ATF5, CD44, COL1A1, COL6A3, CXCL10, CYP19A1, DUSP5, FOXC1, GNA15, GZMB, HOXC6, ID2, IER3, IL6, IL9, IL15, IL13RA2, IL1R1, IL2RA, JUN, JUNB, LMNA, MUC1, PCGF2, PRAME, RASSF4, RRAD, SOCS2, SOCS3, TNFRSF8, TXN, WT1
Proliferation of connective tissue cells	.0007	HGF, CCND2, CD44, CDKN1A, IL6, IL15, PDGFRA, SOCS3
Proliferation of lymphocytes	.0001	ADRB2, IL2RA, STAT1, STAT5A, CD44, CD274, CDKN1A, TRA@, TRD@, EBI3, IL6, IL15, SERPINA1, THY1
Signaling of cells	.0000	IL6, IL15, IL26, IL2RA, CCL5, CCL8, CCL17, CCL22, CD97, CXCL10, GJB2, LILRB2, TNFAIP6, TNFRSF11A, TXN
Transcription of gene	.0008	JUN, NFIB, WT1, FOXC1, STAT1, STAT5A, NFKBIA, HGF, AMPH, ASCL1, ATF3, CD44, DUSP4, EHF, IL6, SOCS3
Canonical pathways		
NF-κB signaling	.0005	TNFRSF11A, PDGFRA, NFKBIA, TNFAIP3, IL1R2, CARD10, TRA@, IL1R1, TRD@, TLR8
JAK/Stat signaling	.0204	SOCS3, STAT1, STAT5A, CDKN1A, SOCS2
IL-6 signaling	.0010	IL6, IL1R1, IL1R2, NFKBIA, CYP19A1, JUN, COL1A1, TNFAIP6
IL-9 signaling	.0017	IL9, SOCS3, STAT1, STAT5A, SOCS2
Cytotoxic T lymphocyte-mediated apoptosis of target cells	.0339	GZMB, TRA@, TRD@
Hepatic fibrosis/hepatic stellate cell activation	.0005	HGF, COL1A1, COL3A1, STAT1, IL1R1, CCL5, PDGFRA, CCR7, IL6, IL1R2
IL-15 production	.0437	IL15, IL6, STAT1

Genomic copy number changes are correlated with mRNA expression of target genes

To describe target genes that are deregulated by changes in genomic copy number, we performed a genome-wide integrative analysis using the GEP data of the 29 microdissected HRS cell samples and matching aCGH profiles as published previously.[18] A selection of target genes is shown in Figure 2 highlighting gene alignments in the chromosomal regions most commonly affected by copy number changes. In agreement with the published literature, we confirmed overexpression of *REL* in 2p16.1-gained cases,[26] overexpression of *CD274* in 9p21.3-gained cases,[26,27] and decreased expression of *TNFAIP3* in 6q23.3-deleted cases in keeping with the previously described tumor suppressor gene function of *TNFAIP3* in HL.[6] Moreover, we identified novel correlations of *MLL* expression with 11q23.3 deletion, *FOXO3* expression with 6q23.3 deletion, *TNFRSF17* expression with 16p13.13 gains, *WNT3* expression with 17q21.32 gain, and *TGIF2* expression with 20q11.23. The complete list of 216 significantly correlated genes is provided in supplemental Table 4.

GEP is correlated with primary treatment outcome in CHL

To discover differences in gene expression profiles related to clinical treatment outcomes, we compared 15 primary treatment success cases with 14 primary treatment failure cases. All 29 patients were homogeneously treated with ABVD or ABVD-like chemotherapy, and primary treatment failure was defined as progression or relapse at any time after initial therapy. Using this approach of comparing clinical extremes, we found 957 probe sets to be significantly differentially expressed (raw $P < .05$; supplemental data: Comparison gene lists). Of these probe sets, 413 probe sets were up-regulated and 544 probe sets were down-regulated. Using the top 200 differentially expressed genes for hierarchical clustering, we found clear separation of the cases into 2 clusters highly enriched for treatment successes and treatment failures (Figure 1B). When characterizing the differentially expressed genes by Ingenuity Pathway Analysis, we found genes related to macrophage function, blood vessel development, and NF-κB signaling significantly overexpressed in HRS cells of patients whose primary treatments failed (Table 5). Furthermore, we tested published gene signatures for correlation to the defined outcome groups as previously described.[15] In agreement with the findings of the pathway analysis, we found a macrophage signature[28] ($P = .043$) and a panendothelial signature[29] ($P = .029$) in HRS cells to be correlated with primary treatment failure (supplemental Figure 5).

Elevated CSF1R expression is associated with poor treatment outcome

The number of tumor-associated macrophages in the tumor microenvironment of CHL has been shown to be associated with shortened PFS and OS.[30] However, the underlying biology of this outcome correlation remains unclear. Furthermore, lineage-inappropriate expression of CSF1R was found to be characteristic of and functionally relevant in CHL in an earlier study.[31] Therefore, we focused on the correlation of this macrophage-like expression program of HRS cells with primary treatment outcome. Specifically, CSF1R (probe set 203104_at) as part of the macrophage signature was significantly associated with primary treatment

Table 4. Function and involved pathways of genes down-regulated in HRS cells (Ingenuity Pathway Analysis)

	P (adjusted)	Molecules
Function annotation		
Activation of B lymphocytes	.0005	CD19, CD22, CD38, CD180, DOK3, IGHG1, INPP5D, POU2AF1, PTPRC, TNFRSF17
Cell death of lymphocytes	.0003	CASP4, CD27, CDC2, CR2, EZR, ID3, IGF1, IGHM, INPP5D, ITGB1, ITPR3, LCK, MS4A1, NFATC1, PRKCB, PTEN, RAC2, TGFBR2, TNFRSF17
Contact growth inhibition of normal cells	.0031	HMGB1, LCK, METAP2, PTPRC
Antibody response	.0084	BLNK, HMGB1, IGHG1, LY86, POU2AF1, POU2F2, ST6GAL1
Cell cycle progression	.0014	ATM, CCDC5, CCNA2, CCNG2, CD19, CDC2, CDC16, CDKN3, CDKN2C, CENPE, CKAP2, CKAP5, CLU, CUL3, DBF4, E2F5, ESR1, FOXO1, HHEX, HPGD, IGF1, IRS1, ITGB1, KAT2B, KIF11, LCK, LRIG1, MAD2L1, PPP2R5C, PRKCD, PTEN, RHOA, RPA1, SMARCA4, SSBP2, SYK, TF, TTN
Proliferation of leukocytes	.0026	BTLA, CD19, CD37, CD38, CD48, CD180, CLECL1, CR1, CR2, FYN, IGF1, IGHG1, IGHM, INPP5D, IRF8, ITGB1, ITK, LCK, MS4A1, PTEN, PTPRC, TCL1A, TIMD4, TNFRSF17
Transcription	.0074	ATF1, ATM, BACH2, BCOR, BTG2, C19ORF2, CAMK2D, CCNA2, CCNDBP1, CDC2, CDKN2C, CREM, CXORF15, DHX15, E2F5, ELF1, ELK3, ELL3, ESR1, ESRRG, FLI1, FOXO1, HHEX, HMGB1, ID3, IGF1, IL16, ILF2, IRF8, ITGB1, JAZF1, JMJD1C, KAT2B, KLF12, LCK, MALT1, MAML3, MDFIC, MED21, MED30, MEF2C, MYBL1, NFATC1, NFATC3, NFYB, NRIP1, POU2AF1, POU2F2, PPP3CA, PRKACB, PRKAR2B, PRKCB, PRKCD, PTEN, RASA1, RCOR1, REL, RHOA, SET, SMARCA4, SOX8, SP3, SYK, TAF5, TGFBR2, THOC4, TNFRSF17, TOM1L1, TRAF5, VAV3, YWHAZ, ZFP161, ZHX2
Canonical pathways		
B-cell receptor signaling	.0000	CD19, CD22, CD79A, CD79B, BLNK, SYK, POU2F2, PRKCB, PIK3CG, PIK3CA, PTPRC, CAMK2D, NFATC3, PAG1, RAC2, PPP3CA, NFATC1, INPP5D, RRAS2, VAV3, MALT1, PLCG2, PTEN, PIK3AP1
T-cell receptor signaling	.0000	LCK, FYN, NFATC1, PIK3CG, PIK3CA, PTPRC, NFATC3, ITK, PAG1, RASA1, PPP3CA, RRAS2, VAV3, MALT1, PTPN7
PDGF signaling	.0062	PDGFD, PRKCB, INPP5D, PIK3CG, JAK1, RRAS2, PIK3CA, PLCG2, RASA1
Integrin signaling	.0069	ITGB1, ITGAE, PIK3CG, RHOA, PIK3CA, FYN, RHOH, RHOQ, RAC2, WIPF1, RRAS2, TTN, ARPC3, PLCG2, BCAR3, PTEN
Glucocorticoid receptor signaling	.0043	ESR1, HSPA8, HSP90AB1, NFATC1, NFATC3, HMGB1, PIK3CG, SMARCA4, PIK3CA, KAT2B, HLTF, TAF5, PPP3CA, JAK1, POU2F2, TGFBR2, RRAS2, TAF12, PRKACB, NRIP1
IGF-1 signaling	.0068	IGF1, RASA1, PIK3CG, RRAS2, YWHAZ, IRS1, FOXO1, PIK3CA, PRKACB, PRKAR2B,
Insulin receptor signaling	.0083	IRS1, JAK1, PTEN, INPP5D, PIK3CG, RRAS2, FOXO1, PIK3CA, PRKACB, PRKAR2B, FYN, RHOQ
Chemokine signaling	.0182	PLCB4, PLCG2, PRKCB, CFL1, PIK3CG, RHOA, RRAS2, CAMK2D

failure ($P = .010$). To validate this outcome correlation with CSF1R mRNA expression, we performed ISH in an independent patient cohort composed of 166 CHL patients. ISH was successfully performed and interpretable in 132 cases (79.5%). The technical failure rate of 20.5% was because of negativity of the β-ACT positive control and no staining in macrophages and plasma cells in the remaining 34 cases. HRS cells were scored as CSF1R-positive in 63 of the 132 (48%) cases. Representative images of CSF1R ISH are shown in Figure 3A-B. The clinical and pathologic characteristics of the cohort, according to the CSF1R status of HRS cells, are shown in Table 2. CSF1R positivity was significantly correlated with non-nodular sclerosis histologic subtypes ($P = .003$), mixed cellularity in particular ($P = .010$), and the number of tumor-associated macrophages in the microenvironment as assessed by CD68 immunohistochemistry ($P = .030$). All other clinical parameters were equally distributed between $CSF1R^+$ and $CSF1R^-$ cases. Next, we studied treatment outcome correlations of *CSF1R* expression in HRS cells with PFS and OS. The median follow-up time of living patients was 6.9 years. $CSF1R^+$ cases showed inferior PFS ($P = .011$, log rank) and OS ($P = .047$, log rank; Figure 3C-D). Although mixed cellularity histology was linked to CSF1R positivity, mixed cellularity histology alone was not associated with either PFS ($P = .848$) or OS ($P = .738$). When combining CSF1R ISH with CD68 IHC, we were able to define 3 risk groups: low-risk ($CSF1R\ HRS^-$, $CD68^{low}$), high-risk ($CSF1R\ HRS^+$, $CD68^{high}$), and an intermediate-risk group (all other patients). Ten-year PFS rates were significantly different ($P = .0008$, log-rank): 75% (n = 24, low-risk), 42% (n = 56, intermediate-risk), and 19.5% (n = 52, high-risk; Figure 3E-F). In a multivariate Cox regression model, including the combined score and all factors of the International Prognostic Factors Project Score, the combined ISH/IHC score retained prognostic independence for both PFS ($P = .002$) and OS ($P = .05$).

Discussion

Using GEP of microdissected HRS cells in a large number of primary CHL cases, we were able to describe and refine the specific mRNA expression phenotype of the malignant cells involved in CHL. Our findings are broadly comparable with previous literature of GEP and proteomics studies in HL that also helped to establish the biologic link to the related entity primary mediastinal B-cell lymphoma.[8-10,25,32] Although contamination with cellular components of the microenvironment cannot be ruled out during the microdissection procedure, our results are corroborated by these previous studies, and we were able to validate our results by IHC and gene expression integration indicating that we have achieved high HRS cells purity for GEP.

Specifically, we found down-regulation of B-cell lineage genes (eg, *CD19, CD20, CD79A*, and *CD79B*), deregulation of transcription factor networks (eg, *JUN, NFIB, WT1, POU2AF1/BOB1*, and

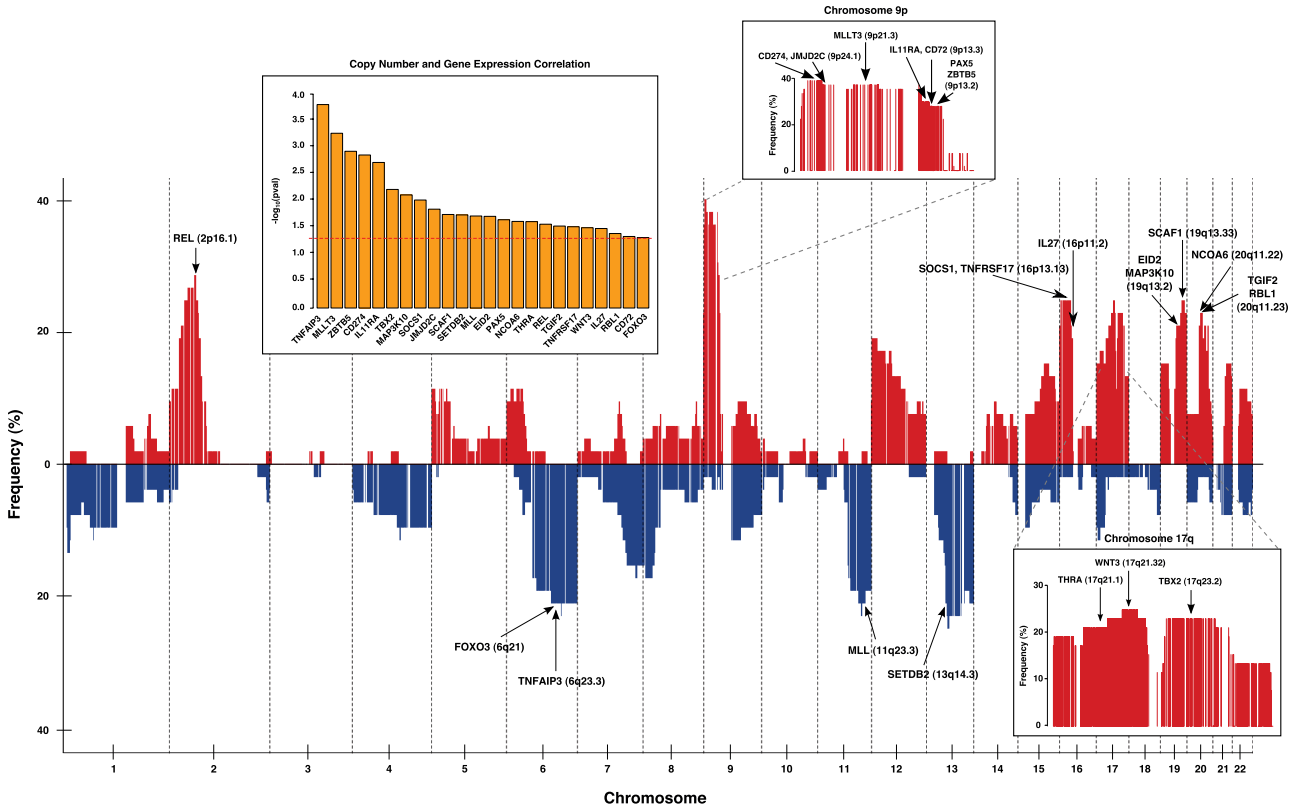

Figure 2. Integrative analysis of copy number and gene expression in microdissected HRS cells (n = 29). Genome-wide copy number data are represented by chromosomal position (x-axis) and the relative frequency of imbalances as shown on the y-axis. Red represents gains; and blue, deletions. A selection of genes in regions of frequent imbalances and with significant correlations between copy number and gene expression are highlighted in the vertical yellow bar plot (the full list of genes is provided in supplemental Table 4). The horizontal red dotted line indicates the *P* value threshold of significance. Target genes are also highlighted on the copy number plot by arrows (cytoband). High resolution views (boxes) of chromosome 9p and 17q are provided to assist in visualizing multiple adjacent genes.

FOXO1), up-regulation of NF-κB and JAK-STAT pathway activators and genes (eg, *TNFRSF11A, PDGFRA, STAT1*, and *STAT5A*), and up-regulation of various chemokines and cytokines (eg, *IL6, IL9, IL15, CCL17/TARC, CCL22/MDC*, and *CX3CL1/fractalkine*). All of these genes and signatures were identified as hallmark alterations of HRS cells.[24] Moreover, comparing these data with signatures derived from cell lines, we found that several genes and pathways were equally regulated, suggesting that findings derived from the study of the existing cell line model systems are partially representative of HL biology. However, the differences in receptor signaling profiles and cytokine/chemokine expression necessitate careful interpretation of cell line data and highlight the need for validation in primary tissue samples. Our comprehensive data on both primary HRS cells and HL cell lines will serve as a repository of deregulated gene expression for future functional studies aiming at experimental perturbation of gene expression in model systems and target identification for novel therapeutic intervention.

We found, for the first time, heterogeneity of gene expression profiles within CHL, suggesting distinct molecular subtypes. One of the identified subtypes (cluster C) was characterized by reduced, but not absent, expression of B cell-specific genes, and interestingly, variable expression of CD20 has been previously described

Table 5. Genes overexpressed in treatment failure according to function and canonical pathways (Ingenuity Pathway Analysis)

	P (adjusted)	Molecules
Function		
Developmental process of hematopoietic progenitor cells	.0122	GATA1, GATA2, WT1, CCND2, TNFRSF11A, CSF1R, IL6ST, INHBA, IRF8
Developmental process of mononuclear leukocytes	.0002	TGFBR2, NFATC1, TNFRSF11A, TNFRSF1A, TNFRSF1B, TNFSF13B, WT1, B4GALNT1, BCL2L11, C3, CSF1R, EOMES, GATA1, GATA2, INHBA, IRF7, IRF8, ITGA4, LAMP1, LTBP1, LTBR, NCAPH2, NPPA, PRDM1, STAP2
Migration of macrophages	.0296	ITGB1, ITGA4, CSF1R, TLR2
Developmental process of macrophages	.0462	CSF1R, PRDM1, TNFRSF1A, INHBA, IRF7, IRF8
Development of blood vessel	.0050	VCAM1, VASH1, SPARC, TGM2, TIMP2, COL18A1, EPHB4, ETV6, GATA2, INHBA, ITGA4, ITGB1, NPR1, PLCD1, QKI, STAB1, TGFBR2, TNFRSF1A, WT1
Canonical pathways		
NF-κB signaling	.0017	PDGFRB, TNFRSF11A, TNFRSF1A, TNFRSF1B, TNFSF13B, LTBR, PRKCB, TLR2
Role of pattern recognition receptors in recognition of bcteria and viruses	.0003	IRF7, IRF8, TLR2, OAS1, C3, CASP1, CLEC7A
Complement system	.0020	C3, C7, CFD, CFH
Macropinocytosis	.0044	ITGB1, ITGB4, PRKCB, CSF1R, ANKFY1

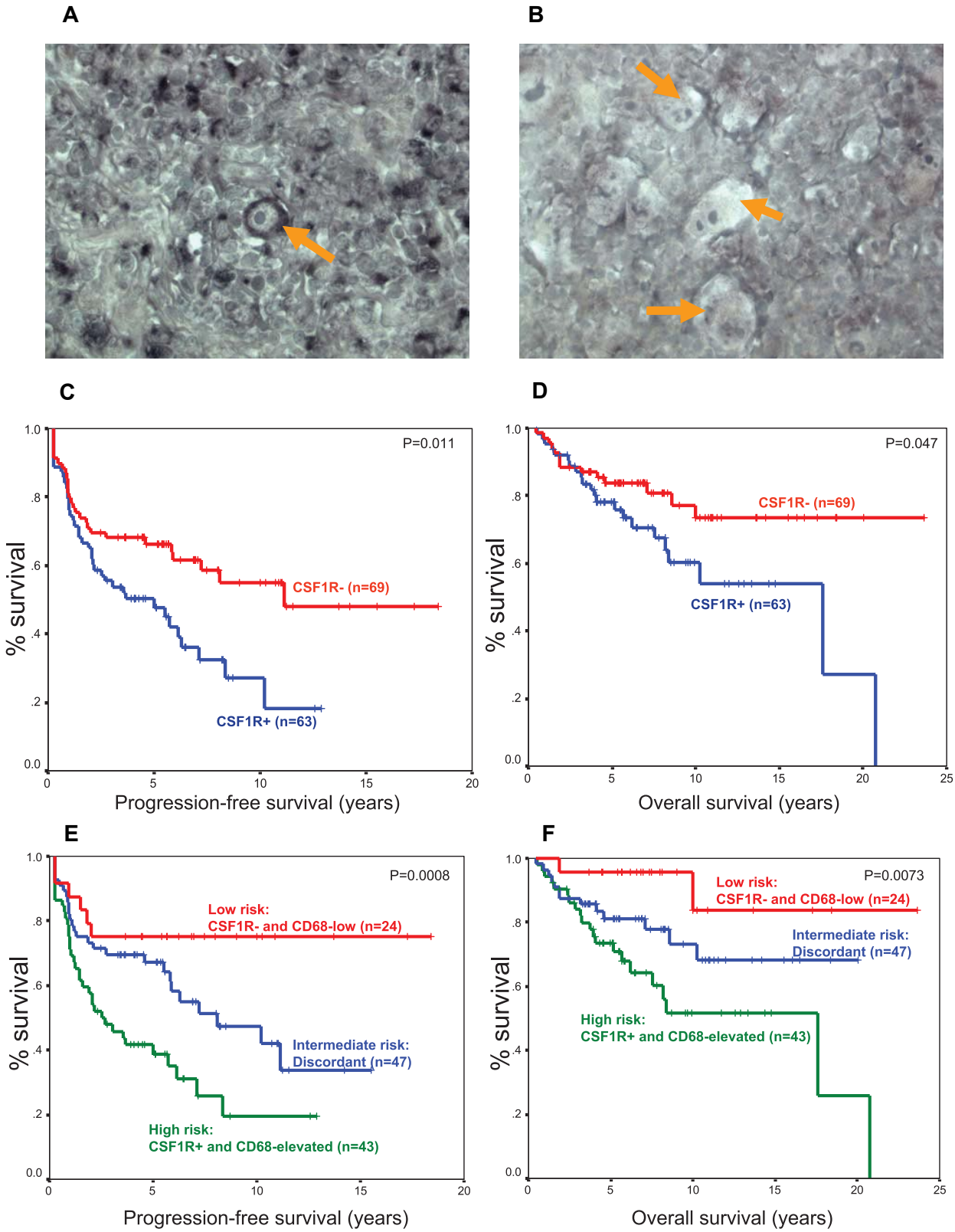

Figure 3. mRNA in situ hybridization in HRS cells identifies patients with inferior PFS and OS in an independent validation cohort (n = 132). (A) A representative CSF1R-positive case is shown highlighting cytoplasmic positivity in a Hodgkin cell (orange arrow) and macrophages in the reactive infiltrate. (B) A representative CSF1R-negative case is shown with no staining in the multinucleated HRS cells (orange arrows). (C) PFS according to CSF1R mRNA in situ hybridization. (D) OS according to CSF1R mRNA in situ hybridization. (E) PFS according to a combined CD68 IHC/CSF1R in situ hybridization score. (F) OS according to a combined CD68 IHC/CSF1R in situ hybridization score.

in ~ 20% of CHL.[33] Furthermore, CD20 positivity has been described as part of a clonotypic B-cell phenotype.[34] Hence, our data support the finding that a subgroup of CHL exists that expresses B-cell antigens on HRS cells and might therefore be targetable by anti-CD20 immunotherapy.[2] Another subtype (cluster A) was characterized by a cytotoxic cell expression pattern, and we

could show that GrB protein expression was high in one index case of this cluster. Our data corroborate the finding that, in a subgroup of cases, HRS cells express cytotoxic granule protein such as TIA-1,[23,35,36] and add further evidence that specific expression patterns resembling T/NK cells might contribute to CHL pathogenesis.[25]

Herein, we present a genome-wide analysis of copy number changes correlated with gene expression levels in primary HRS cells. Using this integrative approach, we were able to identify candidate genes harbored within copy number altered regions that have potential tumor suppressor or oncogene function. Correlations of genomic copy number changes with gene expression have been described previously for *PDL1*, *REL*, and *JAK2*.[26,27] Importantly, we were able to validate this correlation only for *PDL1* and *REL*. Lack of correlation of *JAK2* copy number and gene expression was also described in the 2 HL cell lines L428 and L1236.[37] We also found copy number regulation of the known tumor suppressor genes *TNFAIP3* harbored in the commonly deleted chromosomal region 6q23.2.[6] Furthermore, we identified novel genes that have not been known to be regulated by genomic copy number changes. Among these, we found *IL11RA* as a target gene in the 9p13.13 amplicon. *IL11RA* was found to be overexpressed in microdissected HRS cells in a gene-expression profiling study interrogating 140 genes of chemokines, cytokines, and their receptors.[5] Our data confirm these findings and suggest that copy number regulation of *IL11RA* expression might contribute to altered JAK-STAT signaling activation in HL.[38] Increased expression of *IL11RA* has also been described in prostate cancer.[39]

In addition, we found various target genes that are implicated in transcriptional regulation (*FOXO3, PAX5, TBX2*, and *NCOA6*), including genes involved in histone modification (such as *MLL*, *SETDB2*, *JMJD2C*, and *TGIF2*). In particular, variable expression of B-cell activator *PAX5* and histone demethylase *JMJD2C* have been previously studied in HL.[40,41] Most recently, transcriptional repression of the Forkhead box containing transcription factor *FOXO1* has been identified as an oncogenic mechanism in HL,[42] and *FOXO3* mapping closely to *TNFAIP3* on chromosome 6q was identified as a tumor suppressor gene in other lymphoid cancers.[43,44] Our data suggest that *FOXO3* is another candidate tumor suppressor gene in HL that is often codeleted with *TNFAIP3* in cases harboring 6q deletions.

We investigated, for the first time, correlations of gene expression profiles of HRS cells with clinical outcome. Using a dichotomization approach comparing patients who relapsed or progressed after first-line treatment with patients who entered and maintained a long-term complete remission, we were able to discover gene signatures that were significantly correlated with primary treatment outcome. Of these signatures, we next focused on the macrophage-like expression signature that was overexpressed in HRS cells of patients who progressed or relapsed, because the receptor molecule CSF1R, as a representative of this signature, was recently detected to be highly expressed in most primary tumor samples from patients with HL driven by derepression of a long terminal repeat element. It was also shown that CSF1R receptor engagement led to receptor phosphorylation and induction of proliferation by recombinant CSF-1 in HL cell lines.[31] Moreover, our group recently identified a gene signature of tumor-associated macrophages that was significantly associated with primary treatment failure following standard therapies,[15] and we and others validated by IHC a significant correlation of increased numbers of $CD68^+$ macrophages with inferior survival, suggesting tumor-associated macrophages as a new biomarker for risk stratification in CHL.[45-48] Although the underlying biology of HRS cells interacting with macrophages still remains to be further explored, these studies suggest a link between the abundance of tumor-associated macrophages in HL biopsies and a potential underlying molecular mechanism by which HRS themselves (autocrine) or macrophages (paracrine) support tumor cell growth through CSF1R-mediated signaling. Supportive of this hypothesis, our data demonstrate an association of CSF1R expression on HRS cells with the abundance of macrophages in the microenvironment. It is intriguing to speculate that a macrophage-like differentiation state of HRS cells synergizes with tumor-associated macrophages and that a soluble factor confers chemoattractive, pro-proliferative, and differentiation functions on both HRS cells and macrophages to provide growth advantage and therapy resistance. However, further validation studies are needed to confirm not only the outcome correlation of CSF1R, but also other genes within the macrophage-like signature in HRS cells. Interestingly, in vitro studies using the multi-tyrosine kinase inhibitor BAY 43-9006 (Sorafinib) in HL cell lines showed that Sorafinib induces apoptosis and enhances activity of conventional chemotherapeutics in part through CSF1R inhibition, suggesting that autocrine stimulation contributes to cell autonomous growth in CHL cell lines.[49]

The finding that the number of tumor-associated macrophages and CSF1R expression on HRS cells are correlated with each other, and taken as individual markers, are linked with inferior treatment outcome, respectively, led us to develop a combined score to predict PFS and OS. Our data show that the combination of 2 gene expression features, one derived from the malignant cells and the other from the microenvironment, represents a powerful independent prognostic factor in CHL. This combined approach identifies a sizable proportion of patients who are at high risk for primary treatment failure and death after ABVD-type chemotherapy. Unfortunately, immunohistochemical staining for CSF1R in formalin-fixed, paraffin-embedded tissues was technically challenging; therefore, mRNA-ISH was used for validation purposes. As mRNA-ISH for CSF1R proved technically difficult to perform with a substantial failure rate, this methodology is doubtful to be implemented as a routine diagnostic test and further external validation of these results is needed. However, our data highlight in general the power and robustness of biologically defined phenotypes for outcome prediction. Toward the goal of improved outcome prediction leading to more tailored treatment approaches, biomarker studies using multiparameter predictive models capturing aspects of the HL biology are needed and should be a focus of future studies.

In conclusion, our data refine the gene expression phenotype of primary HRS cells, provide potential target tumor suppressor and oncogenes by integrative analysis, and identify novel gene expression features of HRS cells that are correlated with treatment outcome. In particular, our data suggest CSF1R as a drug target for at-risk HL patients.

Acknowledgments

The authors thank the Centre for Translational and Applied Genomics, Margaret Sutcliffe, and Pat Allard for excellent technical support.

This work was supported by Deutsche Forschungsgemeinschaft (postdoctoral fellowship, C.S.), the Cancer Research Society (Steven E. Drabin fellowship, C.S.), the Michael Smith Foundation for Health Research (C.S.), and the Lymphoma Research

Foundation (C.S.). Operational funds were available through the Canadian Institutes of Health Research (grant 178536, R.D.G.).

Authorship

Contribution: C.S. designed the research, performed GEP experiments, analyzed and interpreted the results, and wrote the manuscript; A.D. performed in situ hybridization experiments and analyzed results; T.L. and F.C.C. analyzed GEP data; P.F. interpreted pathology results; A.T. performed GEP experiments; L.B. performed laser microdissection; S.P.S. analyzed and interpreted GEP results; J.M.C. provided and interpreted clinical data; A.v.d.B. designed the research and analyzed in situ hybridization results; and R.D.G. designed the research, interpreted results, and wrote the paper.

Conflict-of-interest disclosure: The authors declare no competing financial interests.

Correspondence: Christian Steidl, Department of Experimental Therapeutics, Centre for Lymphoid Cancer, British Columbia Cancer Agency, 675 West 10th Avenue, Vancouver, BC V5Z 1L3, Canada; e-mail: csteidl@bccancer.bc.ca.

References

1. Younes A, Bartlett NL, Leonard JP, et al. Brentuximab vedotin (SGN-35) for relapsed CD30-positive lymphomas. *N Engl J Med.* 2010; 363(19):1812-1821.
2. Younes A, Oki Y, McLaughlin P, et al. Phase 2 study of rituximab plus ABVD in patients with newly diagnosed classical Hodgkin lymphoma. *Blood.* 2012;119(18):4123-4128.
3. Kanzler H, Kuppers R, Hansmann ML, Rajewsky K. Hodgkin and Reed-Sternberg cells in Hodgkin's disease represent the outgrowth of a dominant tumor clone derived from (crippled) germinal center B cells. *J Exp Med.* 1996;184(4): 1495-1505.
4. Joos S, Menz CK, Wrobel G, et al. Classical Hodgkin lymphoma is characterized by recurrent copy number gains of the short arm of chromosome 2. *Blood.* 2002;99(4):1381-1387.
5. Karube K, Ohshima K, Suzumiya J, Kawano R, Kikuchi M, Harada M. Gene expression profile of cytokines and chemokines in microdissected primary Hodgkin and Reed-Sternberg (HRS) cells: high expression of interleukin-11 receptor alpha. *Ann Oncol.* 2006;17(1):110-116.
6. Schmitz R, Hansmann ML, Bohle V, et al. TNFAIP3 (A20) is a tumor suppressor gene in Hodgkin lymphoma and primary mediastinal B cell lymphoma. *J Exp Med.* 2009;206(5):981-989.
7. Hartmann S, Martin-Subero JI, Gesk S, et al. Detection of genomic imbalances in microdissected Hodgkin and Reed-Sternberg cells of classical Hodgkin's lymphoma by array-based comparative genomic hybridization. *Haematologica.* 2008; 93(9):1318-1326.
8. Rosenwald A, Wright G, Leroy K, et al. Molecular diagnosis of primary mediastinal B cell lymphoma identifies a clinically favorable subgroup of diffuse large B cell lymphoma related to Hodgkin lymphoma. *J Exp Med.* 2003;198(6):851-862.
9. Savage KJ, Monti S, Kutok JL, et al. The molecular signature of mediastinal large B-cell lymphoma differs from that of other diffuse large B-cell lymphomas and shares features with classical Hodgkin lymphoma. *Blood.* 2003;102(12): 3871-3879.
10. Kuppers R, Klein U, Schwering I, et al. Identification of Hodgkin and Reed-Sternberg cell-specific genes by gene expression profiling. *J Clin Invest.* 2003;111(4):529-537.
11. Brune V, Tiacci E, Pfeil I, et al. Origin and pathogenesis of nodular lymphocyte-predominant Hodgkin lymphoma as revealed by global gene expression analysis. *J Exp Med.* 2008;205(10): 2251-2268.
12. Steidl C, Connors JM, Gascoyne RD. Molecular pathogenesis of Hodgkin's lymphoma: increasing evidence of the importance of the microenvironment. *J Clin Oncol.* 2011;29(14):1812-1826.
13. Oudejans JJ, Jiwa NM, Kummer JA, et al. Activated cytotoxic T cells as prognostic marker in Hodgkin's disease. *Blood.* 1997;89(4):1376-1382.
14. Kelley TW, Pohlman B, Elson P, Hsi ED. The ratio of FOXP3+ regulatory T cells to granzyme B+ cytotoxic T/NK cells predicts prognosis in classical Hodgkin lymphoma and is independent of bcl-2 and MAL expression. *Am J Clin Pathol.* 2007;128(6):958-965.
15. Steidl C, Lee T, Shah SP, et al. Tumor-associated macrophages and survival in classic Hodgkin's lymphoma. *N Engl J Med.* 2010;362(10):875-885.
16. Hasenclever D, Diehl V. A prognostic score for advanced Hodgkin's disease: International Prognostic Factors Project on Advanced Hodgkin's Disease. *N Engl J Med.* 1998;339(21):1506-1514.
17. DeVita VT Jr, Costa J. Toward a personalized treatment of Hodgkin's disease. *N Engl J Med.* 2010;362(10):942-943.
18. Steidl C, Telenius A, Shah SP, et al. Genome-wide copy number analysis of Hodgkin Reed-Sternberg cells identifies recurrent imbalances with correlations to treatment outcome. *Blood.* 2010;116(3):418-427.
19. Steidl C, Shah SP, Woolcock BW, et al. MHC class II transactivator CIITA is a recurrent gene fusion partner in lymphoid cancers. *Nature.* 2011; 471(7338):377-381.
20. Irizarry RA, Hobbs B, Collin F, et al. Exploration, normalization, and summaries of high density oligonucleotide array probe level data. *Biostatistics.* 2003;4(2):249-264.
21. Reiner A, Yekutieli D, Benjamini Y. Identifying differentially expressed genes using false discovery rate controlling procedures. *Bioinformatics.* 2003; 19(3):368-375.
22. van den Berg A, Visser L, Poppema S. High expression of the CC chemokine TARC in Reed-Sternberg cells: a possible explanation for the characteristic T-cell infiltrate in Hodgkin's lymphoma. *Am J Pathol.* 1999;154(6):1685-1691.
23. Asano N, Oshiro A, Matsuo K, et al. Prognostic significance of T-cell or cytotoxic molecules phenotype in classical Hodgkin's lymphoma: a clinicopathologic study. *J Clin Oncol.* 2006;24(28): 4626-4633.
24. Kuppers R. The biology of Hodgkin's lymphoma. *Nat Rev Cancer.* 2009;9(1):15-27.
25. Willenbrock K, Kuppers R, Renne C, et al. Common features and differences in the transcriptome of large cell anaplastic lymphoma and classical Hodgkin's lymphoma. *Haematologica.* 2006; 91(5):596-604.
26. Barth TF, Martin-Subero JI, Joos S, et al. Gains of 2p involving the REL locus correlate with nuclear c-Rel protein accumulation in neoplastic cells of classical Hodgkin lymphoma. *Blood.* 2003;101(9): 3681-3686.
27. Green MR, Monti S, Rodig SJ, et al. Integrative analysis reveals selective 9p24.1 amplification, increased PD-1 ligand expression, and further induction via JAK2 in nodular sclerosing Hodgkin lymphoma and primary mediastinal large B-cell lymphoma. *Blood.* 2010;116(17):3268-3277.
28. Martinez FO, Gordon S, Locati M, Mantovani A. Transcriptional profiling of the human monocyte-to-macrophage differentiation and polarization: new molecules and patterns of gene expression. *J Immunol.* 2006;177(10): 7303-7311.
29. St Croix B, Rago C, Velculescu V, et al. Genes expressed in human tumor endothelium. *Science.* 2000;289(5482):1197-1202.
30. Steidl C, Farinha P, Gascoyne RD. Macrophages predict treatment outcome in Hodgkin's lymphoma. *Haematologica.* 2011;96(2):186-189.
31. Lamprecht B, Walter K, Kreher S, et al. Derepression of an endogenous long terminal repeat activates the CSF1R proto-oncogene in human lymphoma. *Nat Med.* 2010;16(5):571-579.
32. Ma Y, Visser L, Roelofsen H, et al. Proteomics analysis of Hodgkin lymphoma: identification of new players involved in the cross-talk between HRS cells and infiltrating lymphocytes. *Blood.* 2008;111(4):2339-2346.
33. Rassidakis GZ, Medeiros LJ, Viviani S, et al. CD20 expression in Hodgkin and Reed-Sternberg cells of classical Hodgkin's disease: associations with presenting features and clinical outcome. *J Clin Oncol.* 2002;20(5):1278-1287.
34. Jones RJ, Gocke CD, Kasamon YL, et al. Circulating clonotypic B cells in classic Hodgkin lymphoma. *Blood.* 2009;113(23):5920-5926.
35. Krenacs L, Wellmann A, Sorbara L, et al. Cytotoxic cell antigen expression in anaplastic large cell lymphomas of T- and null-cell type and Hodgkin's disease: evidence for distinct cellular origin. *Blood.* 1997;89(3):980-989.
36. Asano N, Kinoshita T, Tamaru J, et al. Cytotoxic molecule-positive classical Hodgkin's lymphoma: a clinicopathological comparison with cytotoxic molecule-positive peripheral T-cell lymphoma of not otherwise specified type. *Haematologica.* 2011;96(11):1636-1643.
37. Kluiver J, Kok K, Pfeil I, et al. Global correlation of genome and transcriptome changes in classical Hodgkin lymphoma. *Hematol Oncol.* 2007;25(1): 21-29.
38. Dahmen H, Horsten U, Kuster A, et al. Activation of the signal transducer gp130 by interleukin-11 and interleukin-6 is mediated by similar molecular interactions. *Biochem J.* 1998;331(3):695-702.
39. Campbell CL, Jiang Z, Savarese DM, Savarese TM. Increased expression of the interleukin-11 receptor and evidence of STAT3 activation in prostate carcinoma. *Am J Pathol.* 2001;158(1):25-32.
40. Rui L, Emre NC, Kruhlak MJ, et al. Cooperative epigenetic modulation by cancer amplicon genes. *Cancer Cell.* 2010;18(6):590-605.
41. Foss HD, Reusch R, Demel G, et al. Frequent expression of the B-cell-specific activator protein in Reed-Sternberg cells of classical Hodgkin's disease provides further evidence for its B-cell origin. *Blood.* 1999;94(9):3108-3113.
42. Xie L, Ushmorov A, Leithauser F, et al. FOXO1 is a tumor suppressor in classical Hodgkin lymphoma. *Blood.* 2012;119(15):3503-3511.

43. Karube K, Nakagawa M, Tsuzuki S, et al. Identification of FOXO3 and PRDM1 as tumor-suppressor gene candidates in NK-cell neoplasms by genomic and functional analyses. *Blood.* 2011;118(12):3195-3204.
44. Obrador-Hevia A, Serra-Sitjar M, Rodriguez J, Villalonga P, Fernandez de Mattos S. The tumour suppressor FOXO3 is a key regulator of mantle cell lymphoma proliferation and survival. *Br J Haematol.* 2012;156(3):334-345.
45. Kamper P, Bendix K, Hamilton-Dutoit S, Honore B, Nyengaard JR, d'Amore F. Tumor-infiltrating macrophages correlate with adverse prognosis and Epstein-Barr virus status in classical Hodgkin's lymphoma. *Haematologica.* 2011;96(2):269-276.
46. Tzankov A, Matter MS, Dirnhofer S. Refined prognostic role of CD68-positive tumor macrophages in the context of the cellular micromilieu of classical Hodgkin lymphoma. *Pathobiology.* 2010;77(6):301-308.
47. Yoon DH, Koh YW, Kang HJ, et al. CD68 and CD163 as prognostic factors for Korean patients with Hodgkin lymphoma. *Eur J Haematol.* 2012;88(4):292-305.
48. Jakovic LR, Mihaljevic BS, Perunicic Jovanovic MD, Bogdanovic AD, Andjelic BM, Bumbasirevic VZ. The prognostic relevance of tumor associated macrophages in advanced stage classical Hodgkin lymphoma. *Leuk Lymphoma.* 2011;52(10):1913-1919.
49. Ullrich K, Wurster KD, Lamprecht B, et al. BAY 43-9006/Sorafenib blocks CSF1R activity and induces apoptosis in various classical Hodgkin lymphoma cell lines. *Br J Haematol.* 2011;155(3):398-402.

2012 120: 3530-3540
doi:10.1182/blood-2012-06-439570 originally published online September 5, 2012

Gene expression profiling of microdissected Hodgkin Reed-Sternberg cells correlates with treatment outcome in classical Hodgkin lymphoma

Christian Steidl, Arjan Diepstra, Tang Lee, Fong Chun Chan, Pedro Farinha, King Tan, Adele Telenius, Lorena Barclay, Sohrab P. Shah, Joseph M. Connors, Anke van den Berg and Randy D. Gascoyne

Blood (print ISSN 0006-4971, online ISSN 1528-0020), is published weekly by the American Society of Hematology, 2021 L St, NW, Suite 900, Washington DC 20036.